stellarator news

Published by Fusion Energy Division, Oak Ridge National Laboratory
Building 9201-2 P.O. Box 2009 Oak Ridge, TN 37831-8071, USA

Editor: James A. Rome Issue 70 July 2000
E-Mail: jar@y12.doe.gov Phone (865) 574-1306 Fax: (865) 574-7624
On the Web at *http://www.ornl.gov/fed/stelnews*

Status of Wendelstein 7-X

Major progress has been achieved since the last report in Stellarator News (Issue 61) in the following areas:

- Completion of essential R&D activities
- Placement of contracts
- Management of running contracts.

In September 1999 the DEMO coil (Fig. 1) was successfully tested. Cryogenic tests with the DEMO cryostat started this Spring.

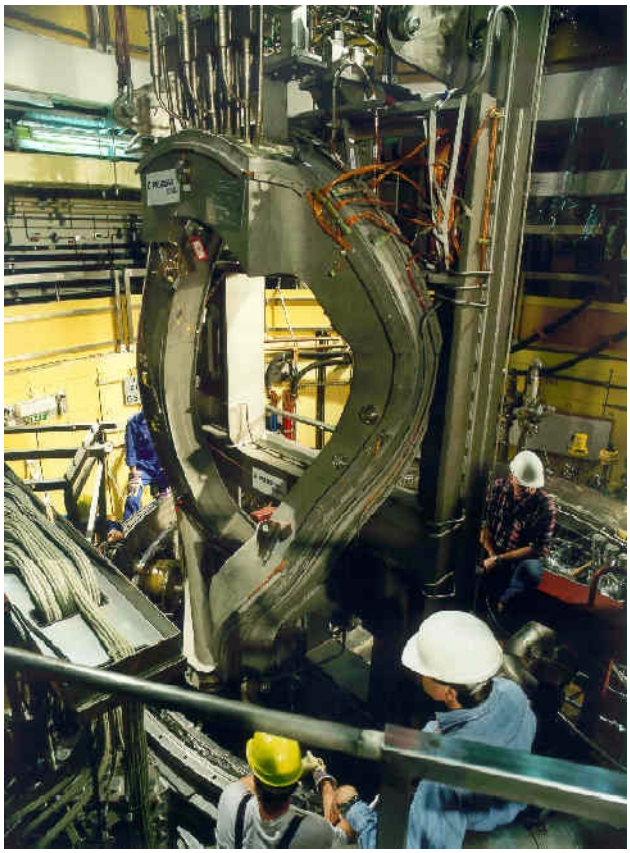

Fig. 1. The DEMO coil during installation in TOSKA. The DEMO coil is mounted on the intermediate frame (By courtesy of FZK).

In addition to these activities a number of major contracts were placed. The contract for the planar coils was concluded with Tesla (GB), the magnet power supply was ordered from ABB (CH), the coil support structure from ENSA (E), the high voltage power supply from the consortium Thomcast/Siemens (CH/D), the power supply for the control coils from JEMA (E), the storage tanks for the liquid cryogenics from Messer Griesheim (D) and the ports from Romabau (CH).

Test of Prototypes

In spring 1999 the DEMO coil, which has been manufactured by Noell/Ansaldo, was mounted in the TOSKA test

In this issue . . .

facility at Forschungszentrum Karlsruhe (FZK) (Fig. 1). After some preparatory tests, the coil became superconducting in June, 1999. The investigations of the DEMO coil were performed in two steps.

First the coil was tested in its self field. Measured quench current of 19.9 kA at 6.4 T and 5 K was in agreement with the expected value calculated from single-strand measurements. Quenches could be detected within fractions of a second and ramp-down of the coil current could be handled safely.

In a second step the DEMO coil was tested in a background field provided by the powerful LCT coil (Large Coil Task). The resulting maximum field at the DEMO coil superconductor reached up to 6.8 T.

During these tests the mechanical behavior of the coil casing, the winding package, and the embedding was tested under Wendelstein 7-X (W7-X) relevant forces. The attractive forces between both coils ranged up to 10 MN. The mechanical distortions and stresses measured were always smaller than the values derived from finite element model calculations. Up to overloads of 114% of the nominal load, the mechanical distortions of the coil were proportional to the applied magnetic forces indicating elastic behavior.

The test-results were summarized in a detailed report. With the successful completion of the electrical, cryogenic and mechanical tests of the DEMO coil the construction principle of the non-planar coils was approved and the W7-X coils were released for manufacture.

Meanwhile the DEMO coil was sent to the Low Temperature Laboratory of Commissariat à l'Energie Atomique (CEA) at Saclay, France, where it will be used to check the test facilities for the series coils.

The DEMO cryostat, representing 1/8 of W7-X, comprises full-sized prototypes of components of the W7-X cryostat (Fig. 2). Only the coils and the support structure are dummies. The assembly of the DEMO cryostat was finished with some delay in August, 1999. Especially, mounting of the superinsulation took more time then expected. After finishing leak tests, the tests of the DEMO cryostat began in September, 1999.

It has been shown, that the plasma vessel and the coil support structure could be displaced sufficiently in order to be able to compensate for thermal expansion effects which occur during heating and cool-down.

Next the distortions of the plasma vessel and the outer shell of the cryostat were measured under different vacuum conditions. The measured distortions correspond to the expected values.

Finally the DEMO cryostat was cooled to 80 K. To avoid excessive tensions in the material the cool down rate was limited to 1 K/h. The measured heat flow rate to the 80 K shield agreed well with the specification. The experience gained during construction, assembly and test of the DEMO cryostat will enter through the specifications of the W7-X cryostat.

Fig. 2. DEMO cryostat ready for testing.

Basic machine (magnet system, cryostat, in-vessel-components)

The nonplanar coils are produced by the Noell/Ansaldo consortium (D/I). The outer shape of the casings were slightly changed to increase their mechanical stability while simplifying the coil support structure. A new fabrication method was introduced by the consortium that allows it to cast complete half-shells of the casings at the required accuracy (Fig. 3). As a result, the time for manufacturing of the coil casings will be reduced.

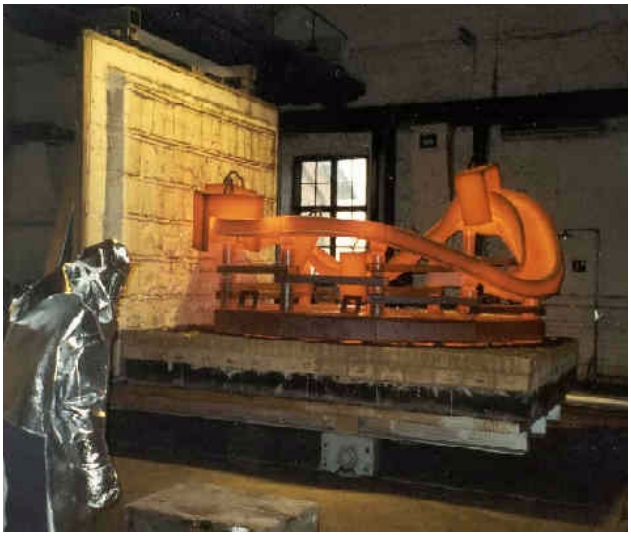

Fig. 3. Half-shell of a nonplanar coil casing. Mechanical stresses are reduced by a glow process. (By courtesy of Noell/Ansaldo).

The planar coils will be produced by Tesla (GB). The contract started in April, 1999. The delivery schedule allows performance of acceptance tests of a major part of the planar coils at Saclay prior to delivery of the nonplanar coils.

Both contractors, Noell/Ansaldo and Tesla, have subcontracted the superconductor to the consortium VAC/EM-LMI (D/I). This company was already in charge for the production of the conductor of the DEMO coil. Meanwhile the first length of 190 m of the superconductor was produced successfully. The first production length will be available for the planar coils in the near future.

The detailed shape of the plasma vessel has been fixed after a number of iterations and considering all physical and technical boundary conditions. During the design of the vessel a compromise had to be found to keep the plasma vessel sufficiently away from the magnet coils and the plasma. As a result the thickness of the thermal isolation had to be reduced on the expense of increasing the cryogenic losses at the 80 K level from 3 Wm^{-2} to 6 Wm^{-2}.

The tender documents for the plasma vessel, the outer vessel, and the thermal isolation are being prepared. The order for the 309 ports of the cryostat has recently been placed with the Swiss company Romabau.

To protect the plasma vessel against energetic particles from the plasma and the plasma from impurities from the wall, the plasma vessel will be protected with heat resistant surfaces. Three different kinds of surface-protecting elements are used for the target plates (10 MWm^{-2}), the baffle plates (0.5 MWm^{-2}), and the wall (0.1 MWm^{-2}). The geometry of these elements is presently designed on the basis of the (now) fixed shape of the plasma vessel and has to consider requirements from diagnostics and the heating systems. For the wall protection, two prototypes of water-cooled stainless steel panels with B4C coating have been ordered from industry. First samples of B_4C coatings have been analyzed.

Work on operational diagnostics has started at the Plasma Diagnostics Division of IPP in Berlin.

Construction work on the divertor cooling cycle has started and large-diameter pipes and the main heat exchangers have been installed.

Three powerful turbomolecular pumps from different suppliers, which are required for the evacuation of the plasma vessel, have been tested in a magnetic field environment. The tests revealed that operation is limited to a magnetic induction of only 3 to 7 mT.

ECRH system

Electron cyclotron resonant heating (ECRH) will be the main heating system of W7-X, especially at the beginning of the experiment. ECRH for W7-X will deliver a microwave power of up to 10 MW at 140 GHz in steady state. This power will be generated by 10 gyrotrons with 1 MW of output power each. FZK has taken responsibility for the development of the gyrotron and the supply of the complete ECRH system. Work is being performed in collaboration with EPFL and IPF Stuttgart.

The first prototype gyrotron, which was developed by TTE (F), was completed in October, 1999. It was baked out and passed leakage and voltage tests. This gyrotron has a depressed collector which allows recovery of a part of the input power and increases the efficiency to 45%.

After delivery of the superconducting magnet in the middle of 2000, the gyrotron will be tested at the FZK. The gyrotron test stand allows tests up to 3 minutes at an output power of 1 MW. Most of the components of the test set-up were already designed to be integrated later in W7-X.

Optical beam lines will be used to transmit the microwave power from the gyrotrons to the plasma. The design and production of all components for the beam lines are performed under the responsibility of the Institut für Plasmaforschung (IPF) in Stuttgart. As a first result of these efforts, an optimized concept for the components that takes into account the mechanical stability, thermal load and costs was worked out. At present, a prototype beam line is under construction.

In addition to ECRH, 4 MW of ion cyclotron resonant heating (ICRH) and 5 MW of neutral beam injection (NBI) heating will be provided.

Commissioning of W7-X and start of the scientific operation is aimed for March, 2006.

T. Bräuer, J.-H. Feist and M. Wanner
and the W7-X construction team
Max-Planck-Institut für Plasmaphysik (EURATOM-Association)
D-17491 Greifswald, Germany
E-Mail: torsten.braeuer@ipp.mpg.de
Phone +49-3834-88-2735

Measurement of magnetic islands with tangential CCD cameras during a plasma discharge

Formation of magnetic surfaces is essential for good plasma confinement in helical systems. Measurement of magnetic surfaces, thus, gives an important basis for detailed plasma confinement studies. The magnetic surfaces have been measured in low magnetic fields (about 0.2 T) in conventional plasma confinement devices [1,2]. In low magnetic fields, the terrestrial magnetism can form magnetic islands on rational surfaces, disturbing the detailed magnetic surface measurement and investigation of error fields.

The Large Helical Device (LHD) is a superconducting device which can sustain a high magnetic field in steady state [3]. Figure 1 shows the experimental setup for measuring magnetic surfaces in LHD. We installed a movable electron gun, a high transparency fluorescent mesh and a high sensitivity charge coupled device (CCD) camera after the second experimental campaign. With these, we successfully measured the magnetic surfaces in high magnetic fields (up to 2.75 T). Clear m (poloidal mode number) =1 and 2 magnetic islands were observed as shown in Fig. 2, which indicates the presence of error fields. We could significantly reduce the islands by optimizing the electric currents of twenty normal-conducting coils [local island divertor (LID] coils) installed above and below the LHD cryostat [4].

Considering the islands formed by the error fields, we set up the three LID coil current configurations in which the size of the m =1 island was expanded, moderate and reduced. We have routinely monitored the plasma dynamic behavior and impurity radiation profiles by using tangentially viewing CCD cameras with interference filters [5]. In the former two LID configurations (expanded and moderate island cases), we observed a stripe of the impurity radiation in the start-up phase of plasma discharges. Fig. 3 (a) and 4 (a) show impurity radiation images of carbon ions (CII: 426.7 nm) observed in both configurations, respectively. It is possible that the stripe is ascribed to the ions diffusing along the magnetic field lines on the m =1 magnetic island.

We calculated the three dimensional structure of magnetic field lines on the m =1 magnetic island by a magnetic field analysis code (HSD) [6]. Figure 3 (b) and 4 (b) show the calculated images of the structure as seen from the tangential port in both configurations. The calculated images are in agreement with the measured ones. This suggests that

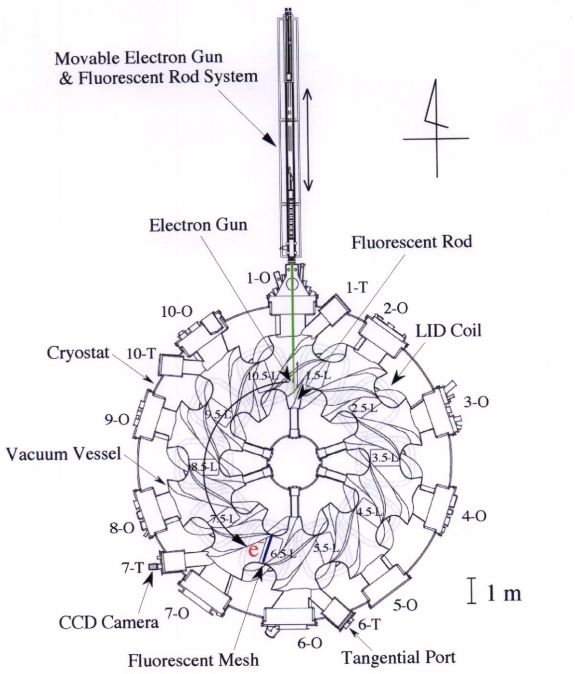

Fig.1. Experimental setup for magnetic surface measurement in LHD.

the presence of magnetic islands can be identified by the tangential camera without the need to install large-scale devices for magnetic surface measurement. In another LID configuration (reduced island case), we could not observe the stripe, which is consistent with the experimental result in the magnetic surface measurement showing the significant reduction of the magnetic island.

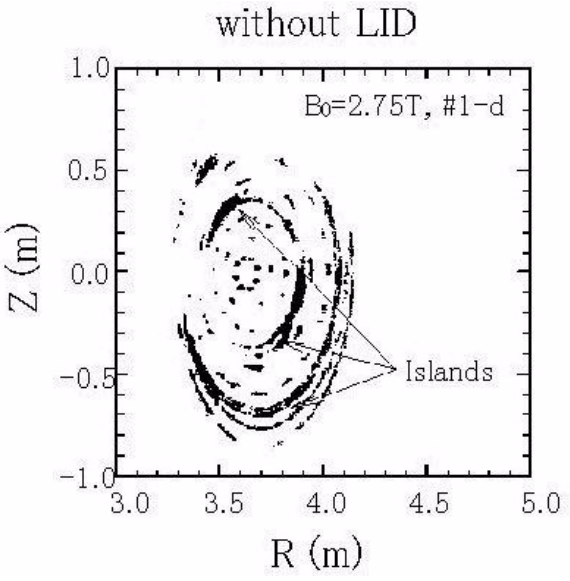

Fig.2. An experimental result of magnetic surfaces in a high magnetic field of 2.75 Tesla without LID coil currents (moderate island case).

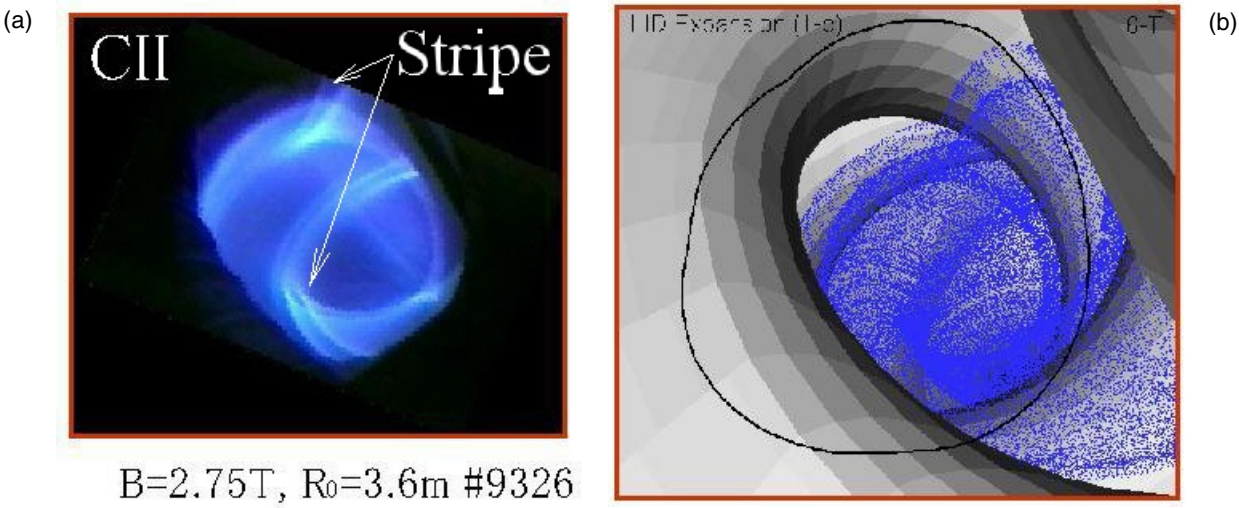

Fig.3. (a) Image of the impurity radiation (CII) observed from a tangential port in the expanded island case, (b) the calculated image of the $m = 1$ magnetic island seen from the tangential port.

In near future, we will try to measure the stripe in detail with a high-speed CCD camera. Impurity radiation images taken by the camera will also contribute the detailed investigation of the impurity transport in magnetic islands and the optimization of the LID coil current configuration for controlling the impurity content in the plasma periphery.

M. Shoji for the LHD Experimental Groups
National Institute for Fusion Science
Toki, Gifu 509-5292, Japan
E-mail: shoji@LHD.nifs.ac.jp

References

[1] R. Jaenicke, et al., Nucl. Fusion **33** (1993) 687.
[2] E Ascasíbar et al., Nucl. Fusion **37** (1997) 851.
[3] A. Iiyoshi, et al., Nucl. Fusion **39** (1999) 1245.
[4] M. Fujiwara, et al., Proc.26th EPS Conf. on Contr. Fus. and Plasma Phys. (1999).
[5] M. Shoji, et al., J. Plasma Fusion Res. SERIES 3 (to be published).
[6] K. Yamazaki, et al., Fusion Eng. and Des. **20** (1993) 79.

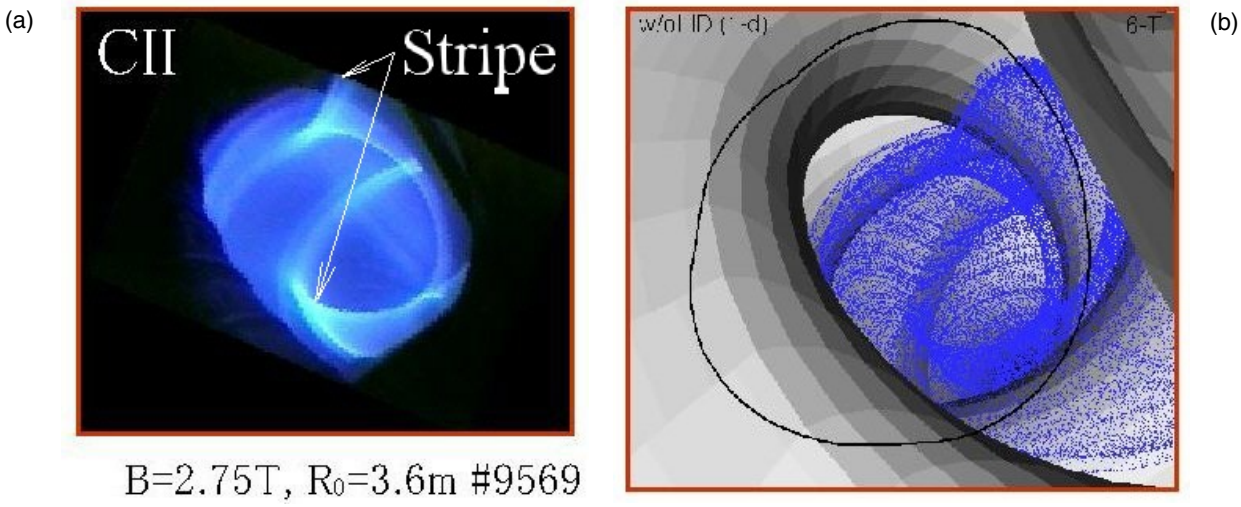

Fig.4. (a) Image of the impurity radiation (CII) observed from a tangential port in the moderate island case, (b) the calculated image of the $m = 1$ magnetic island seen from the tangential port.

Photon counting CCD detector as a tool of x-ray imaging

A new technique of soft x-ray imaging with a soft x-ray photon counting CCD camera has been developed on the Compact Helical System (CHS) and the Large Helical Device (LHD). There are two different operational modes in the soft x-ray CCD camera, image mode and photon counting mode, that can be selected by changing the photon flux. When the flux of the soft x-rays is low enough, about one photon per pixel per frame, the amount of charge in each pixel of the CCD created by the individual x-ray photons is proportional to the energy of the x-rays (photon counting mode). Therefore, the x-ray energy spectra can be obtained by counting the number of photons at given intensity in the photon counting mode.

When the flux of soft x-rays is much higher than the level for the photon counting mode, the intensity of each pixel is proportional to the total x-ray radiation power, and this is called the imaging mode.

Soft x-ray CCD camera system

The photon counting soft x-ray CCD camera system consists of pinholes, Be filters, a shutter and a soft x-ray CCD camera as shown in Fig.1.

The soft x-ray CCD camera used in this diagnostic is Princeton Instruments SX-TE/CCD-1024SB with TEK 1024 × 1024D frame transfer back illumination CCD detector. Since half of the CCD is used as a storage area, the imaging area has 1024 × 512 pixels. Each pixel of the CCD detector is fabricated on special silicon with size of 24 mm × 24 mm. To reduce the dark current, the CCD detector is cooled down to –40°C using multistage Peltier devices.

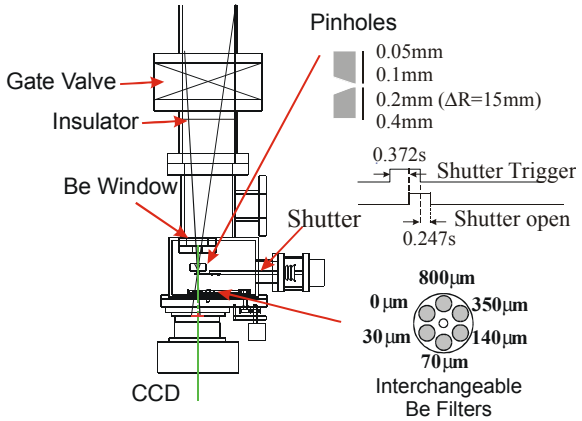

Fig. 1. Schematic of the soft x-ray CCD camera optical assembly as installed on LHD.

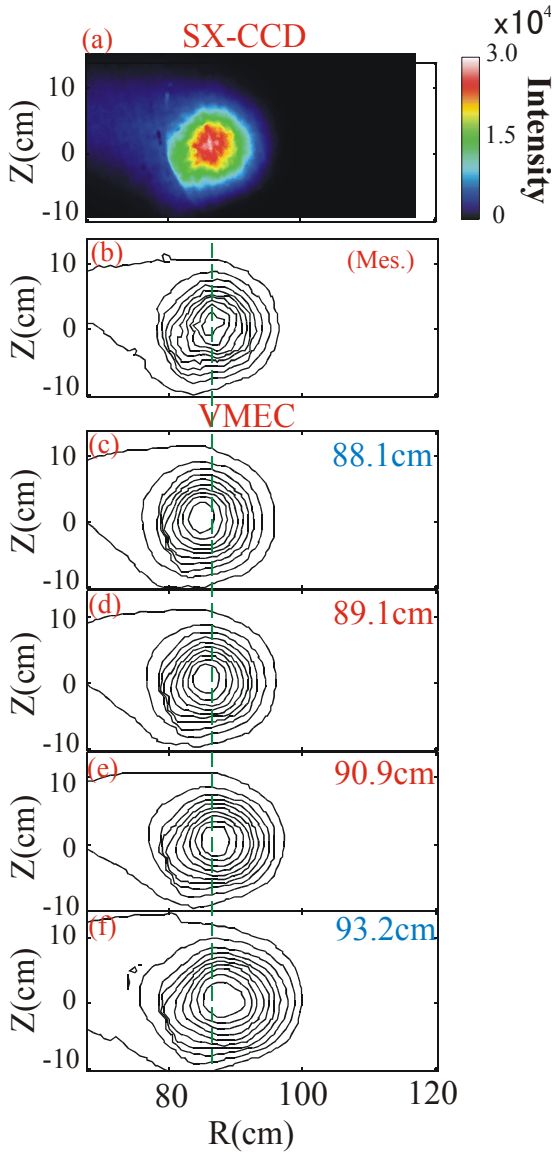

Fig. 2. (a) A tangential soft x-ray image and (b) its contour plot measured by using soft x-ray CCD camera with vacuum magnetic axis R_{axv} = 88.1 cm; and the contour plots of soft x-ray calculated using the VMEC code with four different magnetic axis (c) 88.1 cm, (d) 89.1 cm, (e) 90.9 cm, and (f) 93.2 cm.

Four sets of variable pinholes are installed to adjust the flux of x-rays. A 12-mm-thick tantalum mask with a V-shape hole of 0.5 mm diameter is installed in front of the pinhole plate to prevent high-energy x-rays with energy above 30 keV. Six Be filters with different thickness are installed between the pinhole plate and the CCD detector. The flux of soft x-rays is adjusted to the level used for the imaging mode or the photon counting mode, by changing the combination of pinhole size and Be filter thickness.

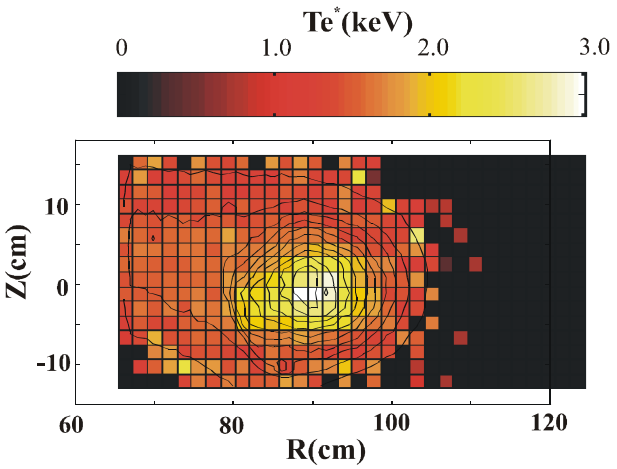

Fig. 3. Two-dimensional profiles of electron temperature measured using the x-ray CCD camera in photon counting mode.

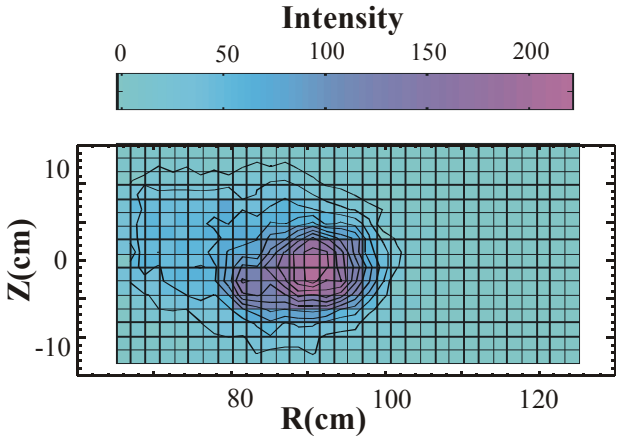

Fig. 4. Two-dimensional profiles of Ti K-α (4.76 keV) radiated intensity.

The tangential soft x-ray image has been measured using the soft x-ray CCD camera in imaging mode with good spatial resolution in both CHS and LHD. Since the total emission of x-rays is considered to be constant on a magnetic flux surface, the shape of magnetic flux surface can be reconstructed from the soft x-ray image. The Shafranov shift of the plasma magnetic axis is derived from the best fit of the measured intensity contour of soft x-ray emission to that calculated with various pressure profiles using an equilibrium code.

We describe one example of analysis on how to derive the magnetic axis of a CHS plasma by using the soft x-ray CCD camera. The target plasma for neutral beam injection (NBI) is produced by electron cyclotron heating (ECH) for t = 25~45 ms and NBI is injected from t = 40 to 140 ms. Figure 2 (a) and (b) show the tangential soft x-ray image and its contour plot measured using the soft x-ray CCD camera with a pinhole diameter of 0.3-mm and a Be filter 10-mm-thick. Figure 2 (c)-(f) show contour plots of soft x-ray image calculated with the three dimensional free boundary equilibrium code VMEC for four different finite beta, 0.0% (R_{ax} = 88.1 cm), 0.2% (R_{ax} = 89.1 cm), 0.5% (R_{ax} = 90.9 cm) and 0.8% (R_{ax} = 93.2 cm). The shift of magnetic axis observed in Fig. 2(b) is in between that calculated for R_{ax} = 89.1 cm (Fig. 2(d)) and R_{ax} = 90.9 cm (Fig. 2(e)). The magnetic axis which gives the best fit to the contour plot observed is 90.3 ± 0.6 cm, and the Shafranov shift is 1.8 ± 0.6 cm.

Two-dimensional profiles of electron temperature and high-Z impurity K-α radiated intensity measurements

Figure 3 shows the two-dimensional profiles of plasma electron temperature derived from energy spectra in 32 ×16 zones. The contour of soft x-ray intensity measured with the CCD camera for a similar discharge is superimposed on the 2-D electron temperature profiles. The integration effect in time is relatively small because the x-ray emission during NBI+ECH phase is much stronger than that during NBI phase.

The 2-D profiles of high-Z impurity radiation intensity can be derived as well as the 2-D electron temperature. Figure 4 shows the 2-D intensity profiles of Ti K-α lines measured with the x-ray CCD camera in photon counting mode. The intensities of Ti K-α line emission are obtained by integrating the intensity of x-rays from 4.65 keV to 4.85 keV. The contribution from bremsstrahlung and the recombination radiation are subtracted. The radial profile of impurities K-α intensity are very peaked at the plasma center because of a sharp increase of emission cross section near the plasma center.

K. Ida, Y. Liang
National Institute for Fusion Science, Japan
E-mail: Ida@nifs.ac.jp, Liang@nifs.ac.jp